



In situ ion exchange preparation of Pt/carbon nanotubes electrode: Effect of two-step oxidation of carbon nanotubes

Sheng Zhang^{a,*}, Yuyan Shao^b, Yunzhi Gao^a, Guangyu Chen^a, Yuehe Lin^b, Geping Yin^{a,**}

^a School of Chemical Engineering and Technology, Harbin Institute of Technology, Harbin 150001, China

^b Pacific Northwest National Laboratory, Richland, WA 99352, USA

ARTICLE INFO

Article history:

Received 17 August 2011

Accepted 18 August 2011

Available online 27 August 2011

Keywords:

Fuel cells

Carbon nanotubes

In situ ion exchange

Oxygen reduction reaction

Electrochemical surface area

ABSTRACT

The in situ ion exchange method has been employed to prepare carbon nanotubes (CNT) supported Pt electrode, in which CNT is functionalized with two-step oxidation, namely electrochemical oxidation and chemical oxidation. X-ray photoelectron spectroscopy (XPS) confirms that two-step oxidation produces more carboxylic acid groups. Transmission electron microscopy (TEM) shows that Pt nanoparticles are highly dispersed on the CNT surface. Electrochemical measurements show that the resultant Pt/CNT electrode treated by two-step oxidation exhibits the largest electrochemical surface area and the highest activity for oxygen reduction reaction (ORR) among the investigated electrodes. This can be attributed to the fact that the two-step oxidation treatment produces more carboxylic acid groups which is the determining factor for Pt loading and dispersion via ion-exchange.

© 2011 Elsevier B.V. All rights reserved.

1. Introduction

Polymer electrolyte membrane (PEM) fuel cells have attracted much attention due to their high-energy efficiency and zero emissions [1–5]. However, the commercialization of PEM fuel cells is severely limited by their high cost [6–11]. Improving the utilization of noble platinum electrocatalysts is considered as an important approach to reducing the cost of PEM fuel cells [12,13]. The electrodes of PEM fuel cells are usually fabricated using the hot-pressing method [14], which is suitable for the fabrication of large-scale membrane electrode assemblies (MEA) and for mass production. However, its major problems include [15]: protons cannot access to Pt nanoparticles isolated from Nafion polymer electrolyte, and Nafion in the catalyst layer tends to wrap some Pt nanoparticles and carbon support, which results in poor electron transport. Therefore, a large amount of Pt electrocatalysts in this electrode prepared via the traditional hot-pressing method are inactive [16]. Alternately, the electrodes prepared by the electrochemical deposition (ECD) can avoid or alleviate the above problems, since the ECD method can deposit Pt catalysts where

both protons and electrons can access [17]. However, Pt nanoparticle sizes synthesized via ECD are large, usually more than 50 nm, which extremely reduces the electrochemical surface area of Pt electrocatalysts [18]. Therefore, Pt specific activity is very low and a large number of Pt electrocatalysts are still required in this electrode.

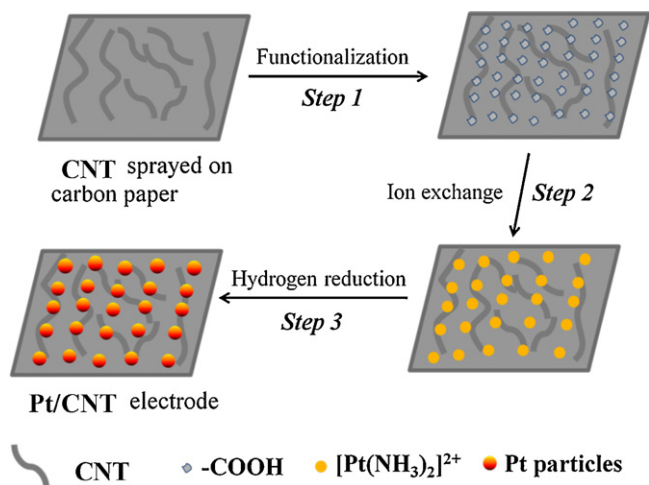
The ion exchange method has been employed to prepare carbon supported Pt catalyst with small particle size [19–21]. However when these catalysts are used in the conventional hot-pressing electrode, it still encounters the same problems mentioned above. Recently, we developed an in situ ion exchange method to prepare a novel electrode for PEM fuel cells, where platinum cation complex was ion exchanged with H⁺ ions of carboxylic acid groups on the carbon support and then reduced to Pt nanoparticles [22,23]. The in situ ion exchange method greatly improved the Pt utilization. However, Pt loading in the resultant electrode was only about 10 mass%, which is not enough for practical application in membrane electrode assemblies (MEA) of PEMFCs [24]. It is known that the ion exchange process undergoes between H⁺ in COOH and Ptⁿ⁺. Therefore, to improve Pt loading, the higher content of COOH is preferred.

Carbon nanotubes (CNT) have been widely investigated as a catalyst support [25–27], which exhibit better performance in terms of catalytic activity and durability than the conventional Vulcan XC-72 [28–31]. In the present study, CNT was sprayed onto carbon paper and then acted as support to load Pt nanoparticles via an in situ ion exchange method. The whole in situ ion exchange process was shown in Scheme 1. More important, a two-step oxidation method, which combined electrochemical oxidation with

* Corresponding author at: School of Chemical Engineering and Technology, Harbin Institute of Technology, No. 92, West Da-Zhi Street, Harbin 150001, China. Tel.: +86 451 86417853.

** Corresponding author at: School of Chemical Engineering and Technology, Harbin Institute of Technology, No. 92, West Da-Zhi Street, Harbin 150001, China. Tel.: +86 451 86413707.

E-mail addresses: zhangsheng1982@hit.edu.cn (S. Zhang), yingphit@hit.edu.cn (G. Yin).



Scheme 1. Illustration of the synthesis process of Pt/CNT electrode: (step 1) functionalization of CNT (step 2) ion exchange between $[\text{Pt}(\text{NH}_3)_2]^{2+}$ and H^+ in $\text{R-COO}^- \text{H}^+$ of functionalized CNT, and (step 3) Hydrogen reduction of $[\text{Pt}(\text{NH}_3)_2]^{2+}$ to Pt nanoparticles.

Table 1
Oxygen-containing functional groups distribution obtained by fitted results of the C1s XPS spectra on CNT based electrodes.

Sample	C–O–C	C=O	COOH
Original	70.55	28.75	1.70
EO-CNT	64.46	21.94	13.60
CO-CNT	61.49	23.96	14.55
TO-CNT	55.12	24.54	20.34

chemical oxidation, was developed to functionalize CNT prior to the ion exchange process. This produced more carboxylic acid groups at the electroactive sites on CNT surface, and more Pt nanoparticles were deposited via the following in situ ion exchange process. The resultant electrode with Pt loading of 16.4 mass% exhibited higher electrochemical surface area (ESA) and catalytic performance towards oxygen reduction reaction (ORR).

2. Experimental details

2.1. Functionalization of CNT-based electrode

CNT-based electrode was prepared as follows. Multi walled CNT (10–20 nm in diameters, 5–15 μm in lengths) and PTFE were mixed with Milli-Q ultrapure water in ultrasonic bath. The obtained ink above was sprayed onto the PTFE-hydrophobized carbon paper with loading of 3.0 mg cm^{-2} at 40°C . Then the electrode with geometric area of $1 \text{ cm} \times 1 \text{ cm}$ was sintered for 30 min at 340°C .

Electrochemical oxidation was performed by 535 potential cycles with the potential range of 0.05–1.4 V (vs. RHE) ($\approx 8 \text{ h}$) and the scan rate of 50 mV s^{-1} in $0.5 \text{ mol L}^{-1} \text{ H}_2\text{SO}_4$ at room temperature. And chemical oxidation was performed by soaking CNT-based electrode in the aqueous solution of 15 mol L^{-1} nitric acid for 48 h at room temperature. The two-step oxidation included two oxidation methods above: the electrode was treated by firstly electrochemical oxidation and then chemical oxidation.

2.2. Preparation of Pt/CNT electrode

The functionalized CNT electrode above was sufficiently washed with Milli-Q ultrapure water to remove the residual solution, and

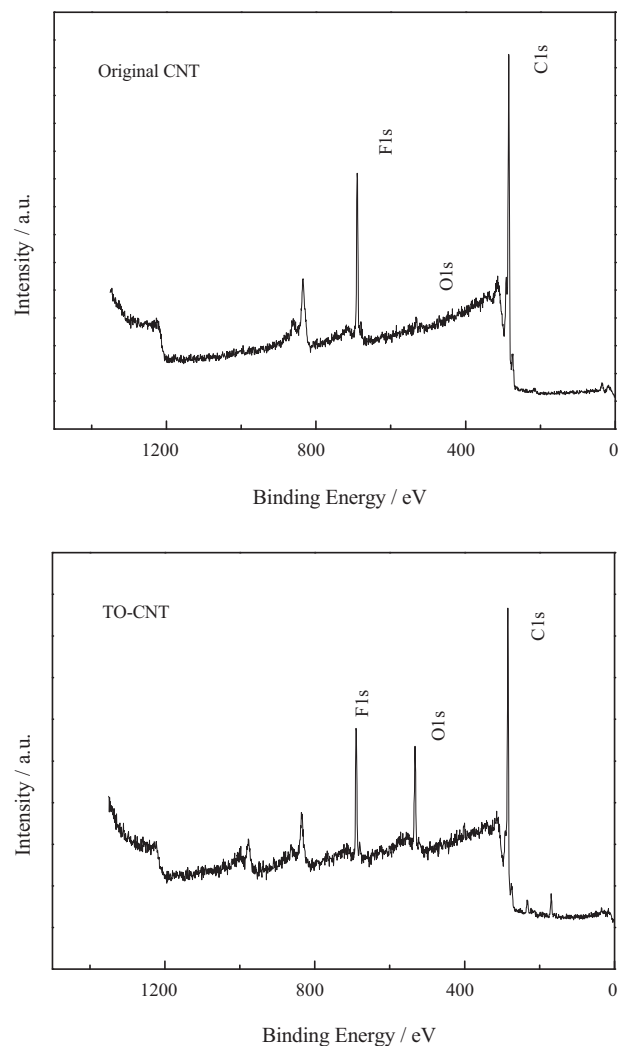


Fig. 1. Survey XPS spectra of original CNT and TO-CNT electrodes.

immersed in $15.0 \text{ mmol L}^{-1} \text{ Pt}(\text{NH}_3)_2(\text{NO}_2)_2$ solution for 48 h. The ion exchange can be tentatively formulated as the following:



The COOH groups were produced on the surface of CNT via the functionalization treatment. And then the electrode was immersed in Milli-Q ultrapure water and stirred for 48 h. The water was refreshed every 8 h to remove the non-ion-exchanged Pt precursor. Then the ion-exchanged Pt ions ($\text{COO}[\text{Pt}(\text{NH}_3)_2]^+$) in the electrode were reduced to Pt nanoparticles in H_2 at 190°C . The electrode was immersed in Nafion solution until the loading was up to 0.36 mg cm^{-2} . Finally, the electrode above was pressed with Nafion membrane at 135°C under a pressure of 5 MPa. The half-membrane electrode assembly was obtained.

2.3. Physical characterization and electrochemical measurements

X-ray photoelectron spectroscopy (XPS) measurements are made using a Physical Electronics Quantum-5600 Scanning ESCA Microprobe. The Al X-ray source operated at 250 W. The sample to analyzer takeoff angle was 45° . Survey spectra were collected at pass energy (PE) of 187.85 eV over the binding energy range 0–1300 eV. Pt/CNT catalysts scraped from the ion-exchanged electrode were characterized by transmission electron microscope (TEM, JEOL JEM-1200EX). Pt loadings in Pt/CNT were determined

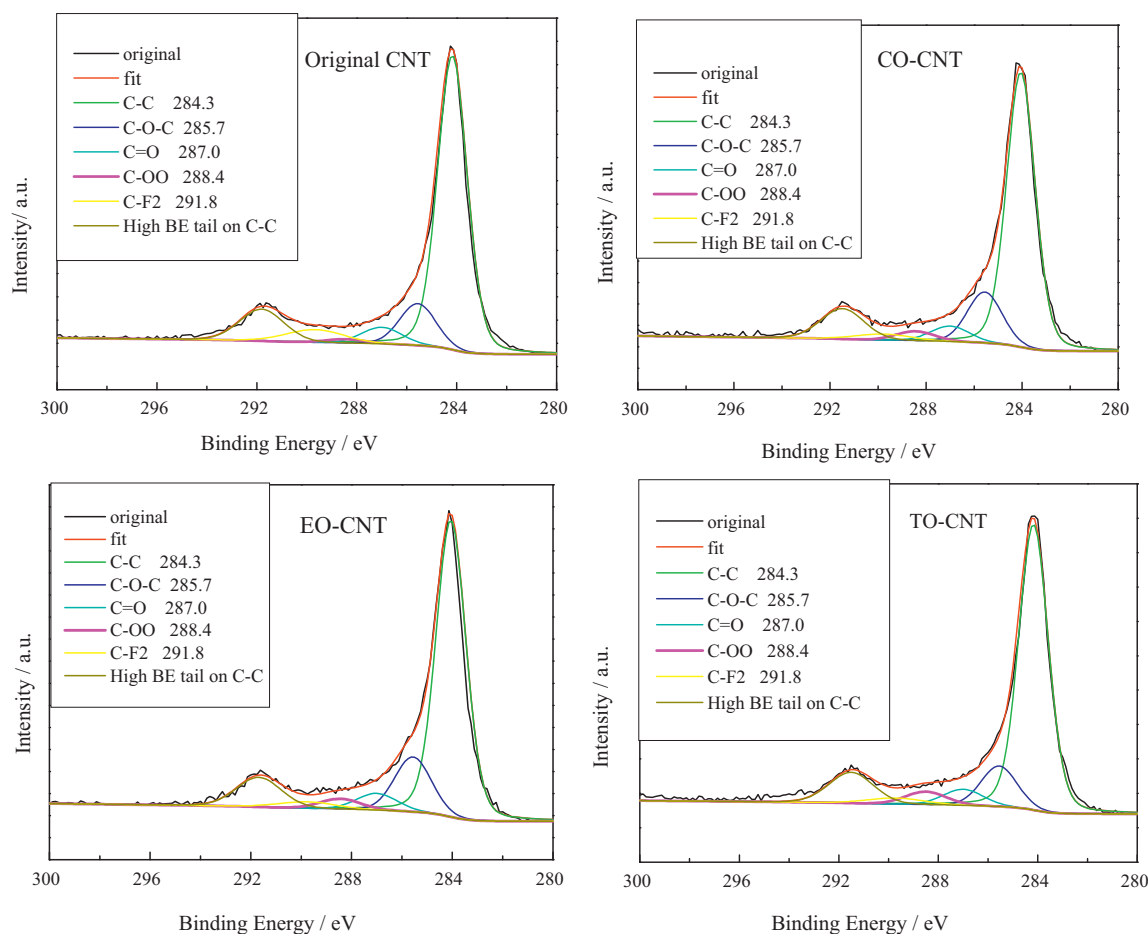


Fig. 2. C1s XPS spectra of original CNT, EO-CNT, CO-CNT, and TO-CNT electrodes.

by thermogravimetric analysis (TGA), which was carried on NET-ZSCH STA449F3 with a heating rate of $10^{\circ}\text{C min}^{-1}$ in an air flow (40 mL min^{-1}).

Cyclic voltammetry (CV) was employed to study electrochemical surface area of Pt/CNT electrode. A reversible hydrogen electrode (RHE) and a Pt foil of 1 cm^2 were used as the reference electrode and the counter electrode, respectively. Measurements were performed at a scan rate of 10 mV s^{-1} . Before all CV experiments, the electrolyte solution was saturated with Ar gas. Oxygen reduction reaction (ORR) was performed in the same electrochemical cell. The working electrode was held vertically in a chamber filled with $0.5\text{ mol L}^{-1}\text{ H}_2\text{SO}_4$ solution. O_2 (30 mL min^{-1}) was supplied to the carbon paper side and the other side was exposed to H_2SO_4 solution. All the tests were conducted at room temperature. All potentials were reported versus the reversible hydrogen electrode (RHE).

3. Results and discussions

The functionalized CNT electrodes are characterized with X-ray photoelectron spectroscopy (XPS). As shown in Fig. 1, compared with the original CNT electrode, the two-step oxidation functionalized electrode (TO-CNT) exhibits much higher O1s peak, indicating that the two-step oxidation functionalization produces a large number of oxygen-containing groups on the CNT surface. F1s peaks shown in Fig. 1 can be assigned to the presence of the PTFE used in the preparation process of the CNT based electrode.

Carboxylic groups on the carbon materials are usually considered as strong exchanger during the ion exchange process which determines Pt loading [32]. Therefore, the information of carboxylic groups generated during the functionalization process is of great importance. Fig. 2 shows high-resolution C1s spectra of the functionalized CNT based electrodes. In the fitted curve, the peak at 288.4 eV is assigned to carboxylic acid groups. The approximate contributions of oxygen-containing functional groups to overall C1s signals are shown in Table 1. The results show that the relative content of carboxylic acid groups on the TO-CNT electrode is more than those on the electrochemical oxidation functionalized (EO-CNT) or chemical oxidation functionalized (CO-CNT) electrode. The highly oxidized groups (COOH) on TO-CNT electrode is calculated to be more than that on EO-CNT electrode (20.34% vs. 13.60%), while the lowly-oxidized species (C–O–C) on the TO-CNT electrode is less than that on EO-CNT electrode (55.12% vs. 64.46%). It has been reported that HNO_3 oxidation could convert surface oxygen-containing groups on carbon materials to more oxidized state species [33]. Therefore, it can be concluded that, for TO-CNT electrode, electrochemical oxidation produces oxygen-containing groups on CNT surface, and the following HNO_3 oxidation converts the lowly oxidized groups (C–O–C) to more highly oxidized groups (such as carboxylic acid groups) [33]. As a result, more carboxylic acid groups are generated on the TO-CNT electrode.

TEM images and Pt nanoparticle size-distribution histograms of Pt/CNT catalysts are shown in Fig. 3. Pt nanoparticles are highly dispersed on the CNT and the averaged Pt nanoparticle sizes for the three Pt/CNT catalysts are calculated to be the same, about 4.0 nm .

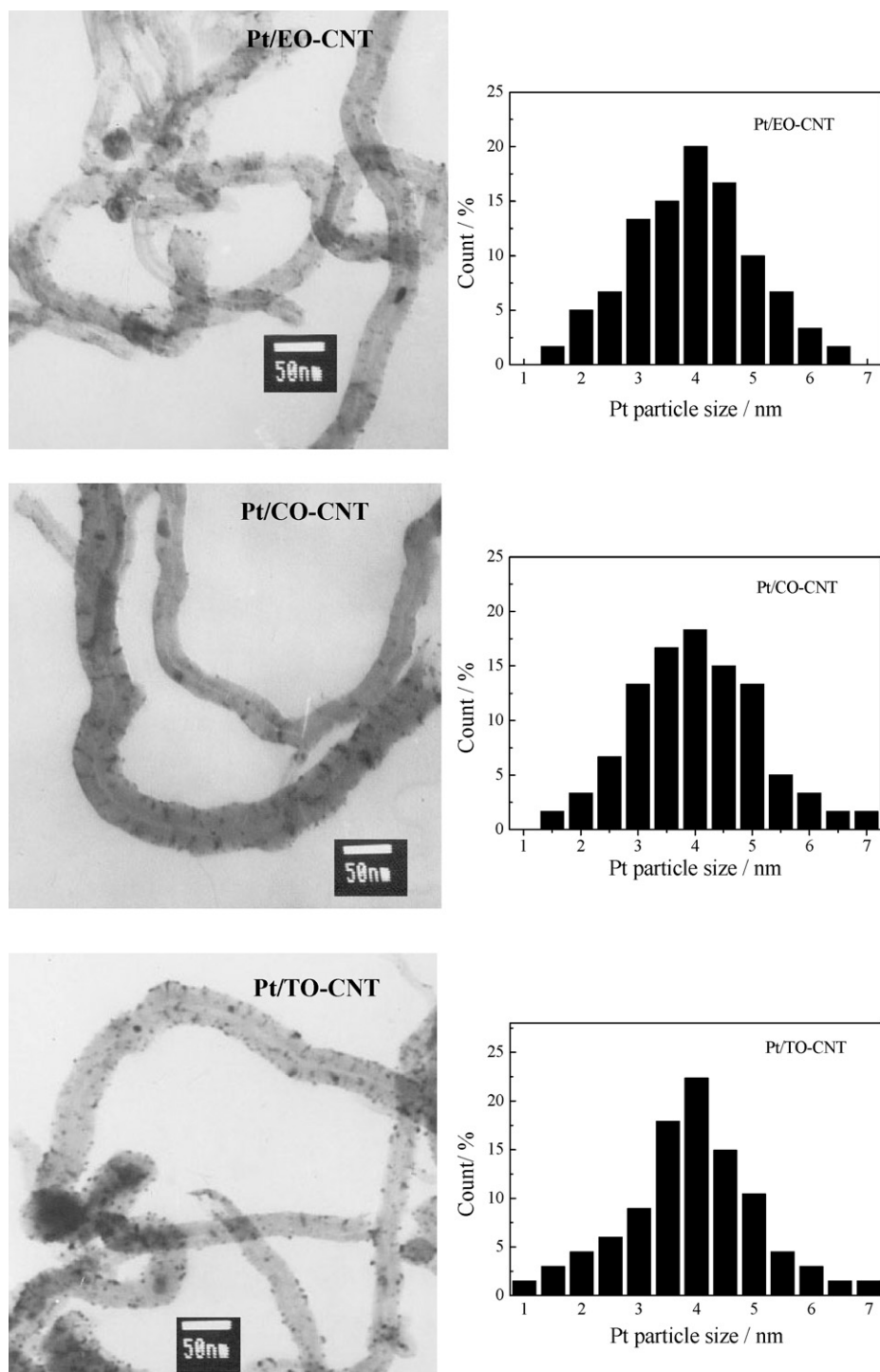


Fig. 3. TEM images and corresponding Pt nanoparticles size distributions of Pt/EO-CNT, Pt/CO-CNT, and Pt/TO-CNT catalysts.

The three catalysts are also characterized by thermogravimetric analysis (TGA), which shows the contents of Pt: 16.4% for Pt/TO-CNT, 11.5% for Pt/EO-CNT and 10.4% for Pt/CO-CNT. Therefore, the two-step oxidation functionalization significantly increases the Pt loading on CNT surface.

Fig. 4 shows cyclic voltammograms (CVs) of resultant Pt/CNT electrodes. A typical hydrogen and oxygen adsorption/desorption behavior on platinum can be clearly observed on all the three samples. Electrochemical surface area (ESA) is one of the most

important parameters for evaluating the performance of PEM fuel cell electrodes [34]: higher ESA means more catalyst sites available for electrode reactions. The ESA can be calculated with coulombic charges of hydrogen adsorption and desorption in CVs:

$$ESA = \frac{Q_H}{Q_C}$$

where Q_H (mC) is the charge transfer for hydrogen adsorption and desorption in the hydrogen region (0.05–0.4 V), and Q_C is 0.21

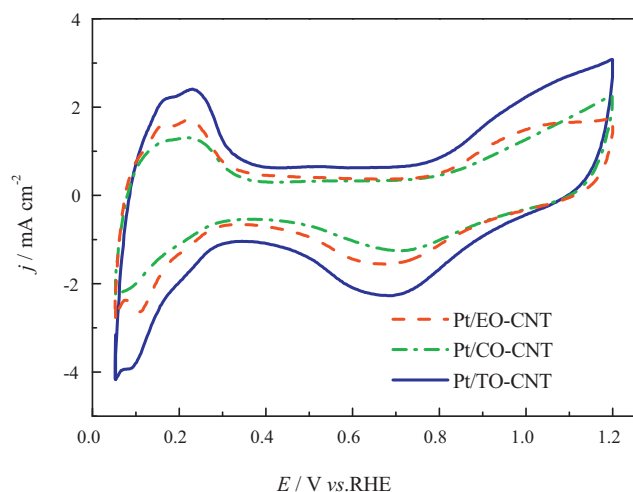


Fig. 4. Cyclic voltammograms on Pt/EO-CNT, Pt/CO-CNT, and Pt/TO-CNT electrodes in the $0.5 \text{ mol L}^{-1} \text{ H}_2\text{SO}_4$ solution, scan rate: 10 mV s^{-1} .

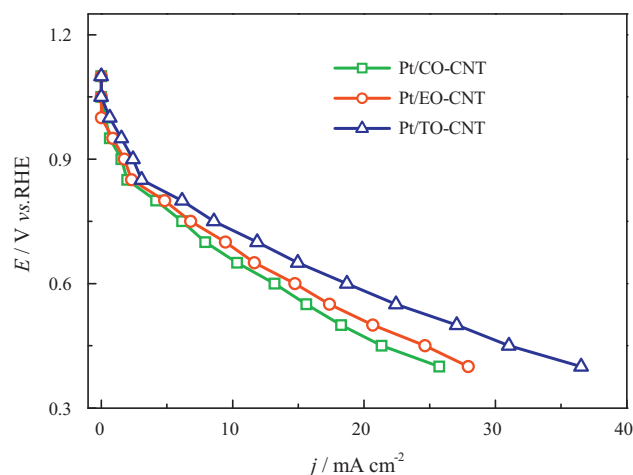


Fig. 5. Polarization curves of oxygen reduction reaction on Pt/EO-CNT, Pt/CO-CNT, and Pt/TO-CNT electrodes. O_2 flow rate 30 mL min^{-1} , $20 \pm 1^\circ \text{C}$, ambient pressure.

(mC cm^{-2}) in the electrical charge constant associated with monolayer adsorption of hydrogen on Pt particles. The results show that the resultant Pt/TO-CNT electrode exhibits the largest electrochemical surface area of 280.3 cm^2 , much higher than Pt/EO-CNT (202.0 cm^2) and Pt/CO-CNT (168.2 cm^2) electrodes.

Since Pt nanoparticle sizes are the same in the three Pt/CNT electrodes, the different ESA of these electrodes can be assigned to the different Pt loadings. For Pt/CNT electrode prepared via ion exchange method, Pt loading is in proportion to the amount of the carboxylic acid groups generated on the CNT surface [19,30]. So the different ESA can be attributed to the different amounts of the carboxylic acid groups on the CNT surface. It has been reported that nitric acid oxidation can introduce carboxylic acid groups only at those initial defects [35]. For Pt/TO-CNT electrode, all the oxygen-containing groups produced by electrochemical oxidation are located at the electrochemical active sites, and the following nitric acid oxidation converts the lowly oxidized species to highly oxidized species (carboxylic acid groups). Compared with other electrodes, TO-CNT electrode has the most amount of carboxylic acid groups at the electrochemical active sites, which results in the most Pt nanoparticles loaded via the in situ ion exchange process. Therefore, Pt/TO-CNT electrode exhibits the largest electrochemical surface area.

Fig. 5 shows oxygen reduction reaction (ORR) polarization curves of the resultant Pt/CNT electrodes. It is obvious that Pt/TO-CNT electrode exhibits higher ORR current densities than Pt/EO-CNT and Pt/CO-CNT electrodes within the whole potential range of $0.4\text{--}1.1 \text{ V}$, which indicates that Pt/TO-CNT electrode has the highest catalytic activity towards ORR among these three electrodes. This is consistent with the results of electrochemical surface areas above.

4. Conclusion

In the present study, a two-step oxidation functionalization of CNT is developed to improve the performance of Pt/CNT electrode prepared via the in situ ion exchange method. Pt/TO-CNT electrode pretreated by the two-step oxidation method demonstrates the largest electrochemical active area and the highest catalytic activity for oxygen reduction reaction, compared with the electrodes treated by electrochemical oxidation or chemical oxidation. This can be attributed to the fact that the two-step oxidation produces more carboxylic acid groups at the electrochemical sites on the CNT surface, which results in more electrochemical Pt nanoparticles loaded in the electrode.

Acknowledgements

This work is financially supported by National Natural Science Foundation of China (Grant Nos. 50872027, 21106024 and 21173062), Ministry of Science and Technology of China (863 program Grant No. 2009AA05Z111), Natural Scientific Research Innovation Foundation in Harbin Institute of Technology (XWQQ5750012411), and Fundamental Research Funds for the Central Universities (HIT.ICRST.2010006).

References

- [1] G. Wu, K.L. More, C.M. Johnston, P. Zelenay, *Science* 332 (2011) 443–447.
- [2] L. Liu, J.-W. Lee, B.N. Popov, *J. Power Sources* 162 (2006) 1099–1103.
- [3] J. Zhang, K. Sasaki, E. Sutter, R.R. Adzic, *Science* 315 (2007) 220–222.
- [4] Y.Y. Shao, S. Zhang, C.M. Wang, Z.M. Nie, J. Liu, Y. Wang, Y.H. Lin, *J. Power Sources* 195 (2010) 4600–4605.
- [5] W.L. Xu, X.C. Zhou, C.P. Liu, W. Xing, T.H. Lu, *Electrochem. Commun.* 9 (2007) 1002–1006.
- [6] S.H. Sun, G.X. Zhang, D.S. Geng, Y.G. Chen, R.Y. Li, M. Cai, X.L. Sun, *Angew. Chem. Int. Edit.* 50 (2011) 422–426.
- [7] S. Zhang, Y.Y. Shao, G.P. Yin, Y.H. Lin, *Angew. Chem. Int. Edit.* 49 (2010) 2211–2214.
- [8] K.P. Gong, F. Du, Z.H. Xia, M. Durstock, L.M. Dai, *Science* 323 (2009) 760–764.
- [9] Z.H. Wen, J. Liu, J.H. Li, *Adv. Mater.* 20 (2008) 743–747.
- [10] S. Wang, S.P. Jiang, T.J. White, J. Guo, X. Wang, *J. Phys. Chem. C* 113 (2009) 18935–18945.
- [11] S. Zhang, Y. Shao, H.-G. Liao, J. Liu, I.A. Aksay, G. Yin, Y. Lin, *Chem. Mater.* 23 (2011) 1079–1081.
- [12] J.W. Guo, T.S. Zhao, J. Prabhuram, C.W. Wong, *Electrochim. Acta* 50 (2005) 1973–1983.
- [13] S.J. Yoo, Y.-H. Cho, H.-S. Park, J.K. Lee, Y.-E. Sung, *J. Power Sources* 178 (2008) 547–553.
- [14] E. Antolini, *J. Appl. Electrochem.* 34 (2004) 563–576.
- [15] X. Wang, M. Waje, Y. Yan, *Electrochem. Solid State Lett.* 8 (2005) A42–A44.
- [16] S.D. Thompson, L.R. Jordan, M. Forsyth, *Electrochim. Acta* 46 (2001) 1657–1663.
- [17] Z.D. Wei, S.G. Chen, Y. Liu, C.X. Sun, Z.G. Shao, P.K. Shen, *J. Phys. Chem. C* 111 (2007) 15456–15463.
- [18] H. Tang, J.H. Chen, Z.P. Huang, D.Z. Wang, Z.F. Ren, L.H. Nie, Y.F. Kuang, S.Z. Yao, *Carbon* 42 (2004) 191–197.
- [19] K. Yasuda, Y. Nishimura, *Mater. Chem. Phys.* 82 (2003) 921–928.
- [20] K. Amine, M. Mizuhata, K. Oguro, H. Takenaka, *J. Chem. Soc. Faraday Trans.* 91 (1995) 4451–4458.
- [21] V. Lordi, N. Yao, J. Wei, *Chem. Mater.* 13 (2001) 733–737.
- [22] Y. Shao, G. Yin, J. Wang, Y. Gao, P. Shi, *J. Electrochem. Soc.* 153 (2006) A1261–A1265.
- [23] J.J. Wang, G.P. Yin, J. Zhang, Z.B. Wang, Y.Z. Gao, *Electrochim. Acta* 52 (2007) 7042–7050.
- [24] S. Thanasilp, M. Hunsom, *Electrochim. Acta* 56 (2011) 1164–1171.
- [25] S. Zhang, Y.Y. Shao, G.P. Yin, Y.H. Lin, *Appl. Catal. B Environ.* 102 (2011) 372–377.
- [26] W.Z. Li, C.H. Liang, W.J. Zhou, J.S. Qiu, Z.H. Zhou, G.Q. Sun, Q. Xin, *J. Phys. Chem. B* 107 (2003) 6292–6299.

- [27] J.J. Wang, G.P. Yin, H. Liu, R.Y. Li, R.L. Flemming, X.L. Sun, *J. Power Sources* 194 (2009) 668–673.
- [28] Y.-T. Kim, T. Mitani, *J. Catal.* 238 (2006) 394–401.
- [29] S. Zhang, Y.Y. Shao, G.P. Yin, Y.H. Lin, *J. Mater. Chem.* 20 (2010) 2826–2830.
- [30] Y.Y. Shao, G.P. Yin, H.H. Wang, Y.Z. Gao, P.F. Shi, *J. Power Sources* 161 (2006) 47–53.
- [31] L. Li, G. Wu, B.-Q. Xu, *Carbon* 44 (2006) 2973–2983.
- [32] Y.F. Jia, K.M. Thomas, *Langmuir* 16 (1999) 1114–1122.
- [33] L.A. Langley, D.H. Fairbrother, *Carbon* 45 (2007) 47–54.
- [34] S. Zhang, Y. Shao, H. Liao, M.H. Engelhard, G. Yin, Y. Lin, *ACS Nano* 5 (2011) 1785–1791.
- [35] J. Zhang, H. Zou, Q. Qing, Y. Yang, Q. Li, Z. Liu, X. Guo, Z. Du, *J. Phys. Chem. B* 107 (2003) 3712–3718.